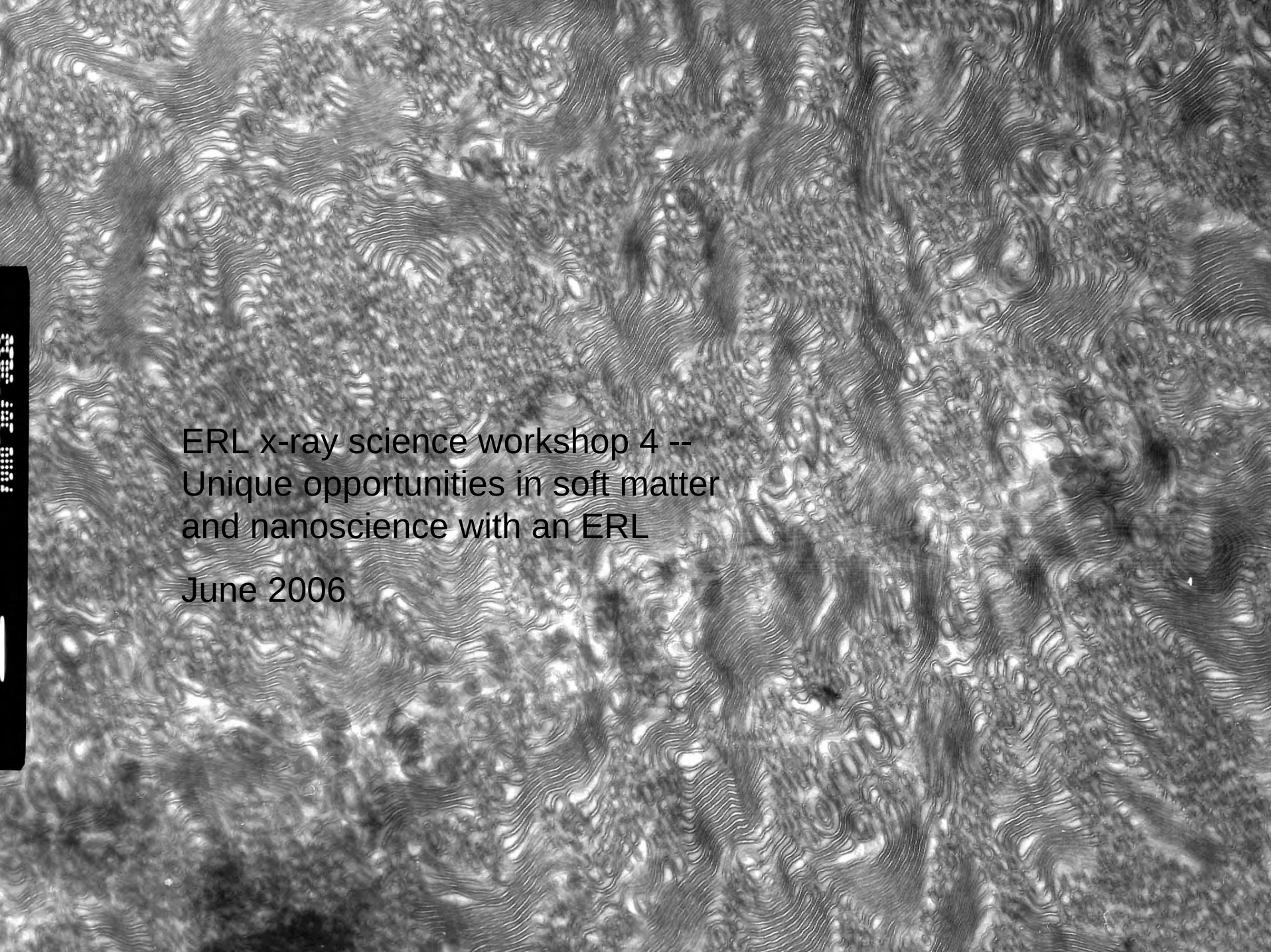

ERL x-ray science workshop 4 -- Unique opportunities in soft matter and nanoscience with an ERL

June 2006

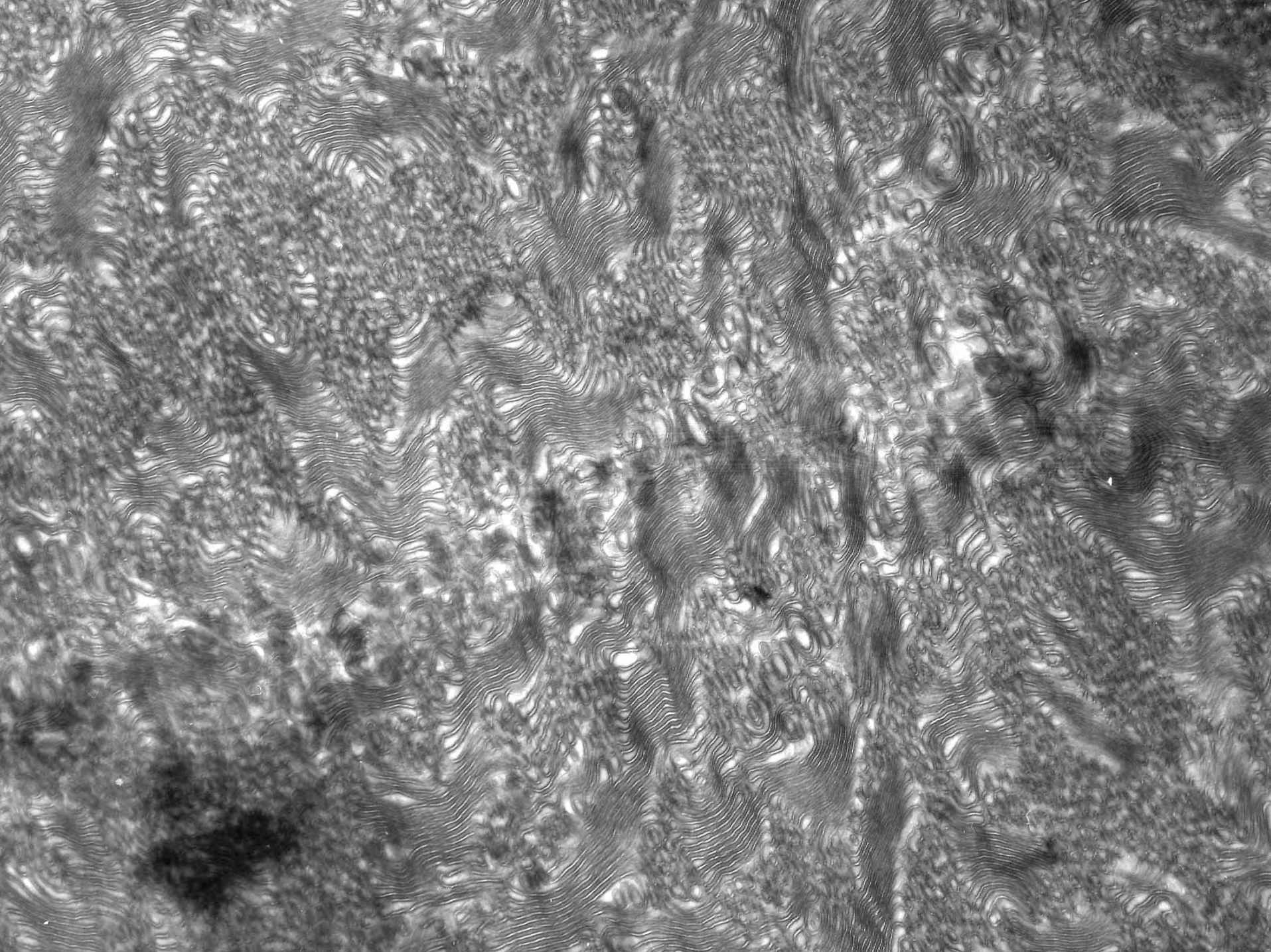

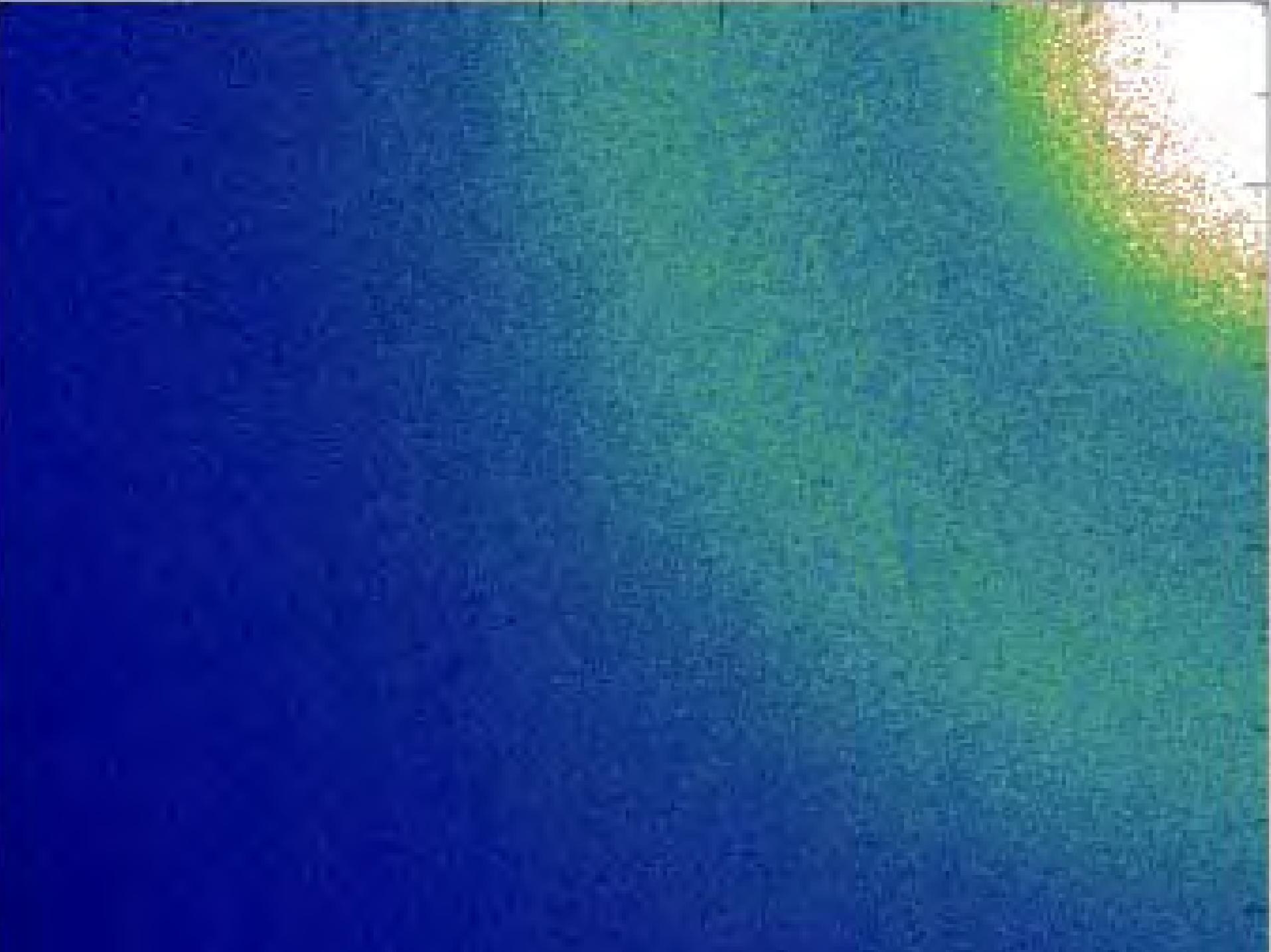

Dynamic x-ray speckle from a concentrated colloidal suspension (R = 170 nm):

QuickTime™ and a
YUV420 codec decompressor
are needed to see this picture.

Recorded at 500 fps and played back at 25 fps.

At the peak, these data represent many more x-rays per pixel per accumulation time than needed to achieve a good intensity autocorrelation function (g2), but even in the low intensity regions, the g2s are measureable in a few seconds.

500 fps is too slow to fully capture the short-time behavior, limited by detector speed, not by photon scattering rate.

Intensity autocorrelation function (g2), calculated pixel-by-pixel and averaged over equivalent pixels for a PSEBS-PS polymer blend.

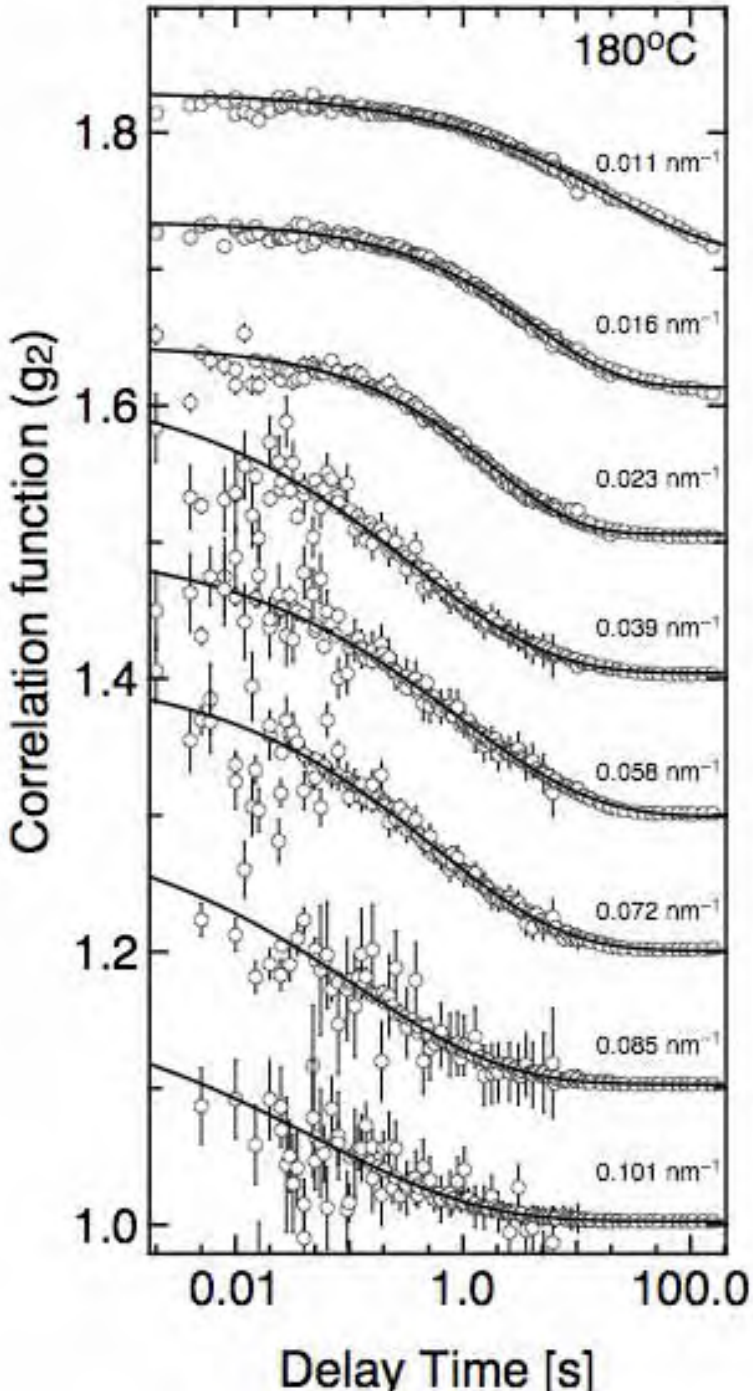

COHERENCE

XPCS requires a (partially) transversely coherent beam.

The role of brilliance is as follows:

The number of transversely coherent x-rays (n_c) is the number passing through an aperture that subtends the solid angle corresponding to the coherence lengths (ξ_x and ξ_y):

$$n_c = B(\pi\sigma_x\sigma_y)(\frac{\pi\xi_x\xi_y}{R^2}) \quad (1)$$

But

$$\xi_x = \frac{\lambda R}{2\pi\sigma_x} \text{ and } \xi_y = \frac{\lambda R}{2\pi\sigma_y} \quad (2)$$

so

$$n_c = B\lambda^2/4. \quad (3)$$

To create a partially transversely coherent beam, slits at the sample should be no more than a few times ξ_x and ξ_y.

COHERENCE (cont.)

When the illuinated sample dimensions exceed the coherence lengths, the speckle contrast (β) is give by the ratio

$$\beta \simeq \frac{\pi \Xi_x \Xi_y}{LM} \tag{6}$$

for monochromatic beam, where Ξ_x and Ξ_y are the effective coherence lengths, incorporating the effect of the detector resolution in addition to the source size.

It may be shown that this regime yields the best statistical signal-to-noise ratio.

And, for pink beam,

$$\beta \simeq \frac{\pi \Xi_x \Xi_y \delta}{LM\Lambda}. \tag{7}$$

COHERENCE (cont.)

XPCS also requires a (partially) longitudinally coherent beam.

The optical path length difference (δ) between x-rays scattered from different parts of the sample should be no more than a few times the longitudinal coherence length [$\Lambda = \lambda(E/\Delta E)$].

For a transmission geometry, there are two contributions to δ:

(1) from the width of the beam in the scattering plane (L):

$$\delta_L = 2L(Q/k)\sqrt{1 - Q^2/k^2} \tag{4}$$

(2) from the sample thickness (W):

$$\delta_W = 2WQ^2/k^2 \tag{5}$$

For monochromatic beam and small angle scattering δ_L and $\delta_W \ll \Lambda$.

PCS is more difficult with x-rays than with light

- There are many fewer photons in beams from even a third-generation synchrotron than from laser sources
- The x-ray scattering cross-section is generally much smaller that the light scattering cross-section.
- As a result, the crucial aspect of an XPCS experiments is generally the signal-to-noise (SNR).

To obtain the best possible SNR

- The source must be as brilliant as possible.
- The beamline optics must preserve brilliance.
- It is helpful to study strongly scattering samples, in a fashion that minimizes possible x-ray sample damage.
- The detector must collect as many x-rays as possible, over as wide an angular range as possible, but with an angular resolution sufficiently fine to (nearly) resolve speckle, on a time scale commensurate with the sample's interesting dynamics.
- Synchrotron and beamline stability is essential

XPCS SIGNAL-TO-NOISE

Consider Jakeman's expression for the SNR in XPCS applied to a pixellated area detector

$$SNR_{pixel} = \beta n \eta \sqrt{T \tau_a} \sqrt{\tau_a F} \sqrt{n_p} \tag{8}$$

where β is the speckle contrast, n is the mean count rate per pixel, η is the detector efficiency, T is the total measurement time, τ_a is the accumulation time, F is the frame rate and n_p is the number of pixels.

Now,

$$n = n_i \Sigma W \Delta\Omega, \tag{9}$$

where n_i is the number of x-rays incident per second, Σ is the cross-section per unit volume (material property), W is the sample thickness, and $\Delta\Omega$ is the pixel solid angle.

So.... there's a factor of

$$\beta n_i \simeq \frac{\xi_x \xi_y}{LM} n_i \simeq n_c = \lambda^2 B/4 \tag{10}$$

contained within in the expression for the XPCS SNR.

It follows that for an ERL beamline with $B \simeq 2 \times 10^{23}$, the SNR would be improved by a factor of about 5000 in comparison to an APS UA beamline with $B \simeq 4 \times 10^{19}$.

XPCS SIGNAL-TO-NOISE (cont.)

Our own XPCS efforts have focussed on using an x-ray area detector.

For an ideally efficient($\eta = 1$), ideally fast ($\tau_a = 1/F$) point ($n_p = 1$) detector, we have

$$SNR_1 = \beta i \sqrt{T/F} \tag{11}$$

So

$$\frac{SNR_{pixel}}{SNR_1} = \eta \tau_a F \sqrt{n_p} \tag{12}$$

For $n_p = 1024 \times 1024$, there's a 1024-fold inprovement in the SNR with an area detector!!

But currently area detectors cannot be read out very fast. For example, for our SMD 1M60 12-bit CCD camera, $\eta \simeq 0.45$, and for $F < F_{max} = 62$ Hz,

$n_p = 1024 \times 1024$,

but for $F > F_{max}$

$n_p = 1024 \times 1024 \times \frac{F_max(1-\tau_f F)}{F(1-\tau_f F_max)}$

where $\tau_f = 840\ \mu$s is the frame transfer time.

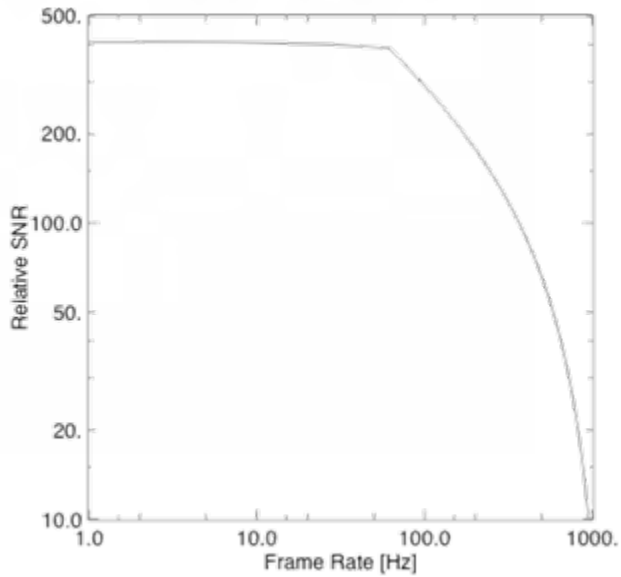

SMD1M60 x-ray area detector

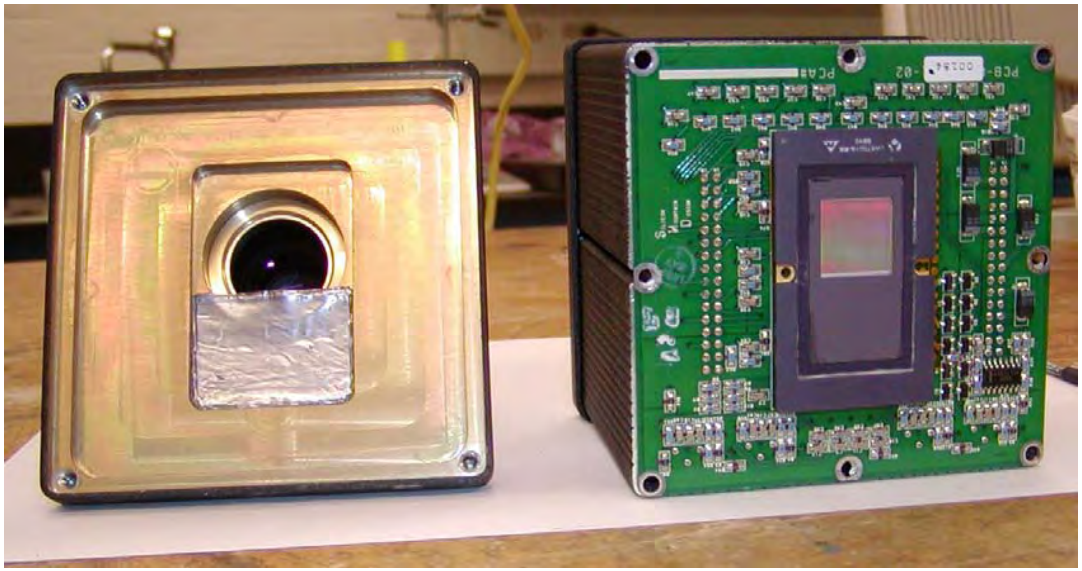

- 1024x1024 14x14 μm^2 pixels -- more would be better [multiple (e.g. 25) detectors]
- 62 Hz full-frame rate--should be MUCH faster at the ERL
- 500 Hz 1/16-frame rate -- should be MUCH faster at the ERL
- counts individual photons -- essential now and at the ERL
- 50% quantum efficiency at 7 keV-- 100% at 12-20 keV at ERL
- inexpensive -- always good, but there should be national/ community effort

X-ray scattering measurements at Beamline 8-ID-I at the Advanced Photon Source at Argonne National Laboratory

Simple optics: apertures, horizontally-deflecting mirror, gravity-water cooled double Ge(111) mono, slits, sample, detector. Only 2 (polished) Be windows in total. Extremely stable. A wonderful Beamline for XPCS, SAXS.
Next big thing: vertical focussing to tune the vertical coherence length.

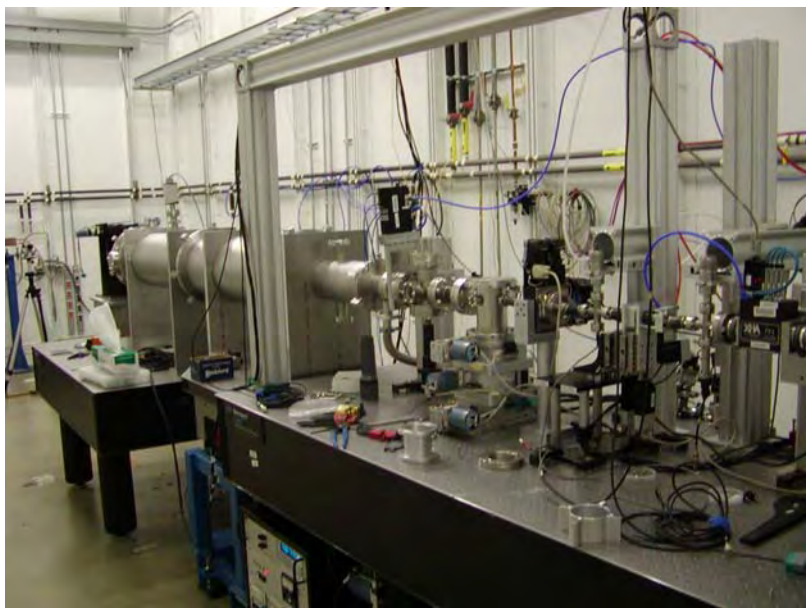

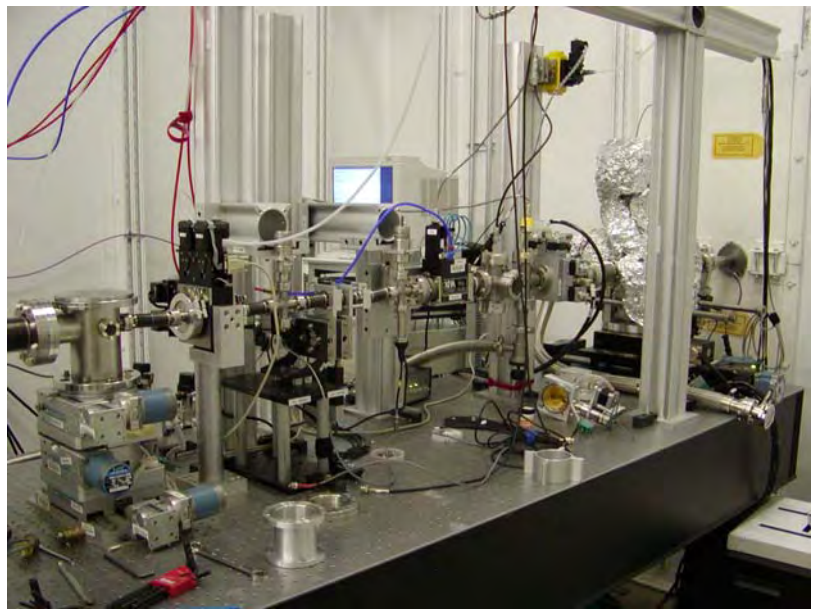

Amphiphilic complex fluids

Amphiphilic molecules possess two (or more) moieties with very different affinities

e.g. soaps, lecithin, block copolymers

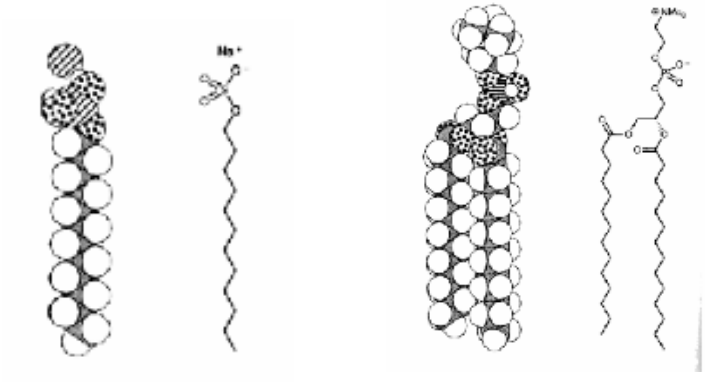

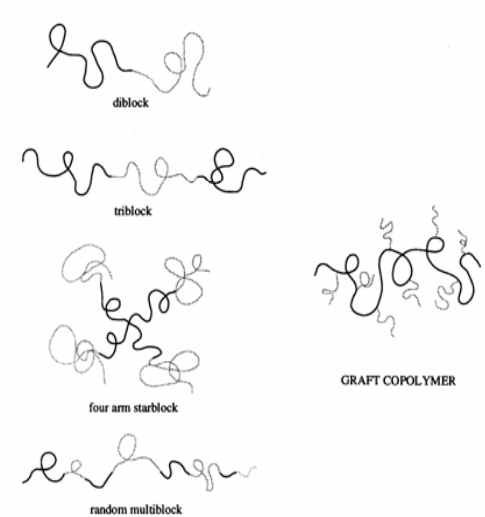

..and organize immiscible fluids

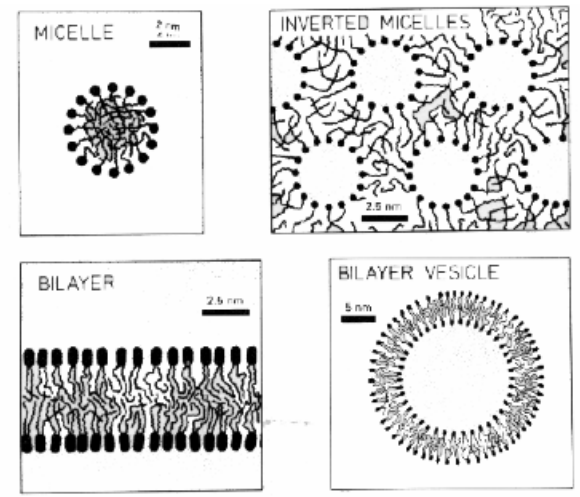

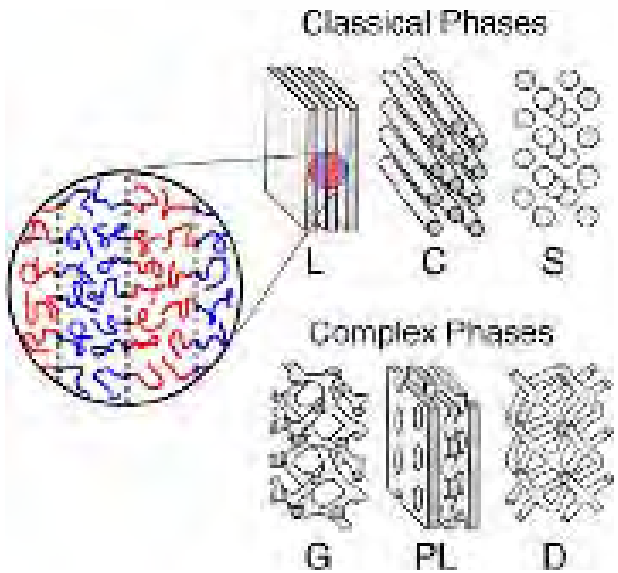

L3 phase microstructure - built from membranes

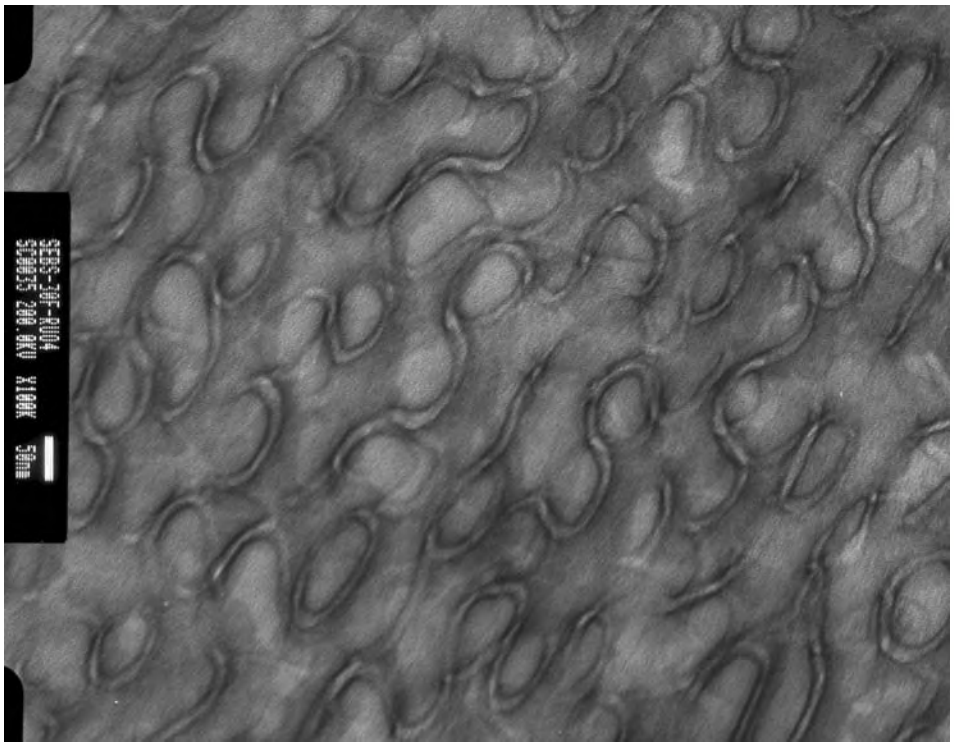

Transmission Electron Microscopy
of Block Copolymer L3 Phase

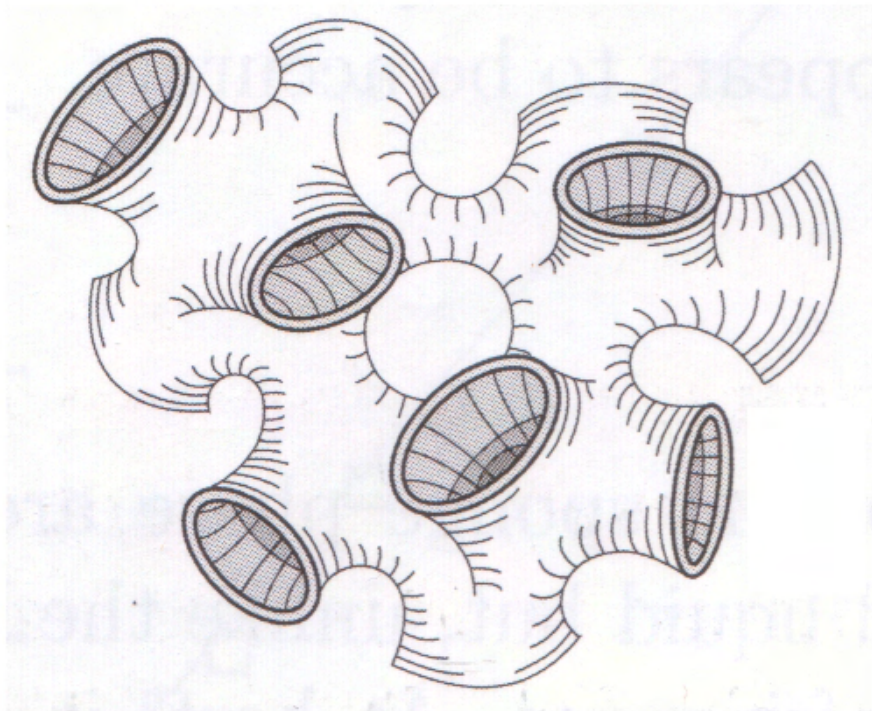

Schematic

SAXS from ϕ=0.20 styrene) triblock copolymer (SEBS) in poly(styrene-ethylene/butylene- polystyrene homopolymer (PS) obtained with the SMD 1M60

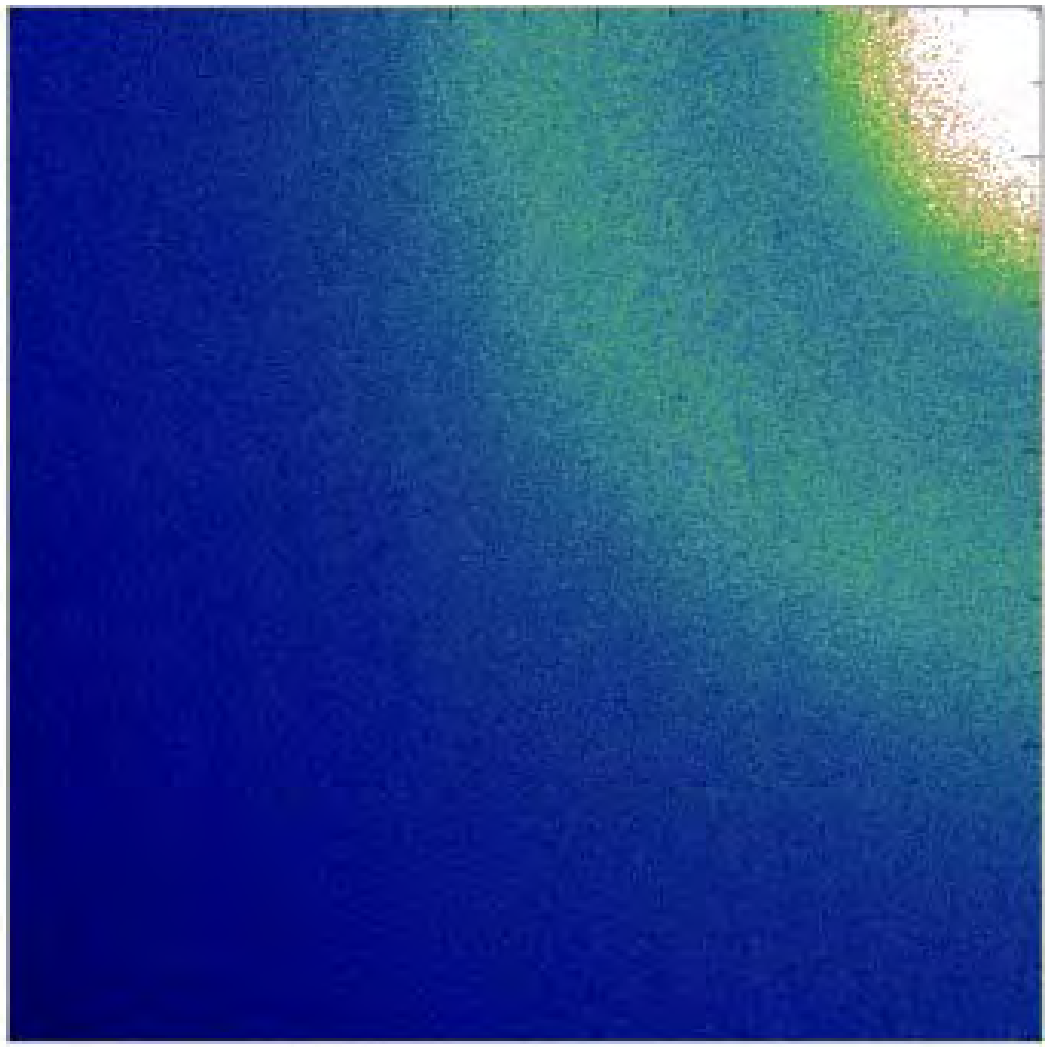

SAXS from SEBS-PS blends:

Large wavevector scattering. Note the >10^5 dynamic range with single-photon-counting SMD 1M60 CCD camera, even with 100 x-ray well-depth.

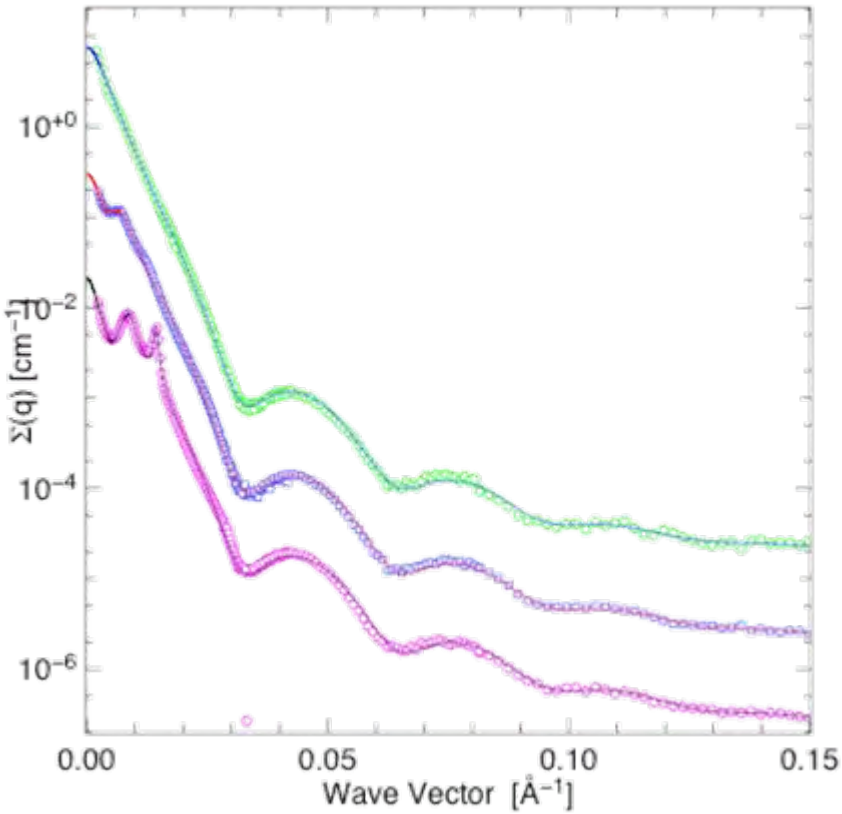

- M_w(SEBS)=87K with M_w/M_n=1.06 and a central P(E/B) volume fraction of 0.7 with PS fractions of 0.15 at each end.
- M_w(PS)=4K, M_w/M_n=1.06
- For all volume fractions studied, there are periodic oscilation in the SAXS intensity at relatively large wavevectors.
- The locations of the oscillation minima relative to zero point unambiguously to a microstructure built from P(E/B) membranes suspended in PS.
- Significantly weaker scattering intensity than colloidal suspensions.

SAXS from SEBS-PS blends (cont.):

Volume-fraction dependence at small wavevectors

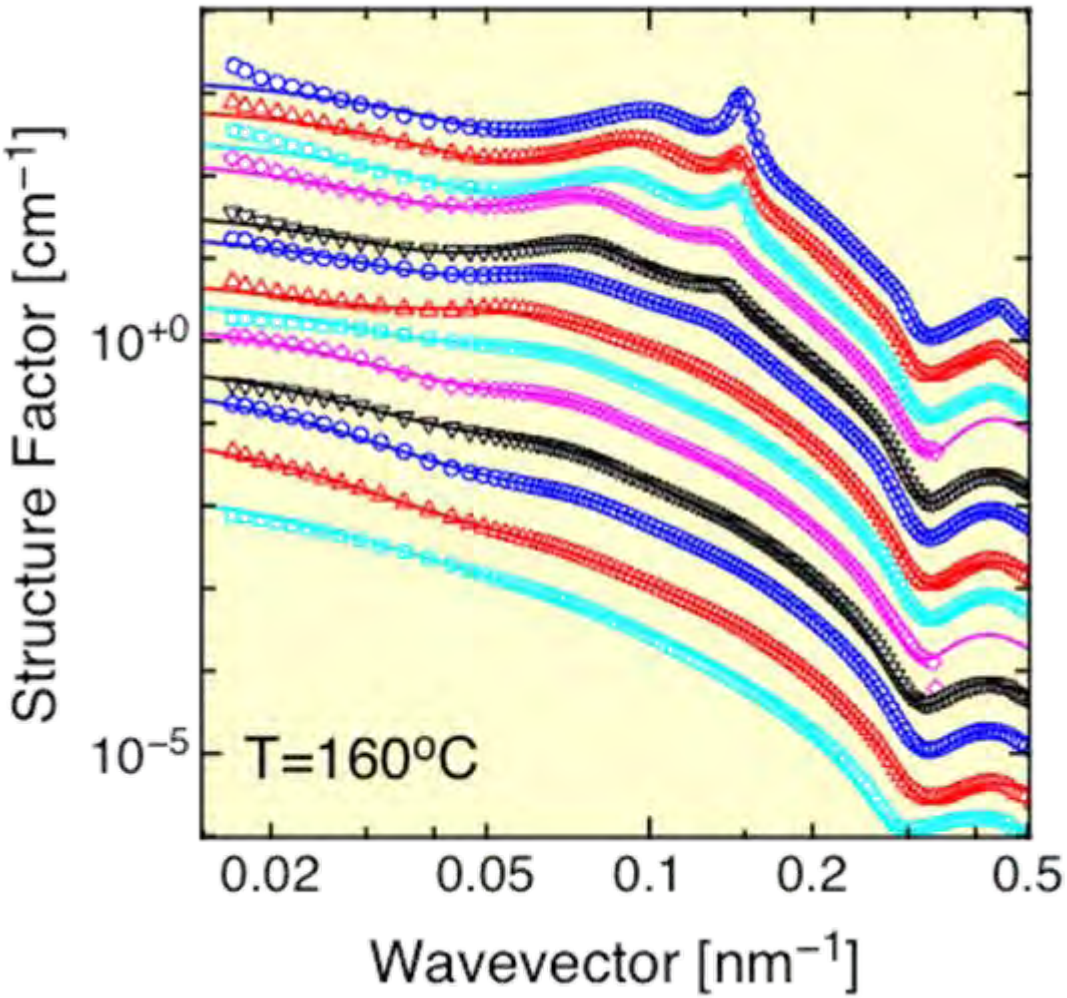

- SEBS volume fractions varying from 0.07 to 0.43.
- At intermediate volume fractions, SAXS consistent with a sponge phase.
- At higher volume fractions, SAXS consistent with sponge/lamellar coexistence
- At low volume fractions, the sponge peak position does not track with the copolymer volume fraction as would be expected in a symmetric sponge phase. We proposed a droplet phase for SEBS volume fractions below about 0.2

Sponge-to-Droplet Transition in TEM: Coexistence at ϕ=0.19

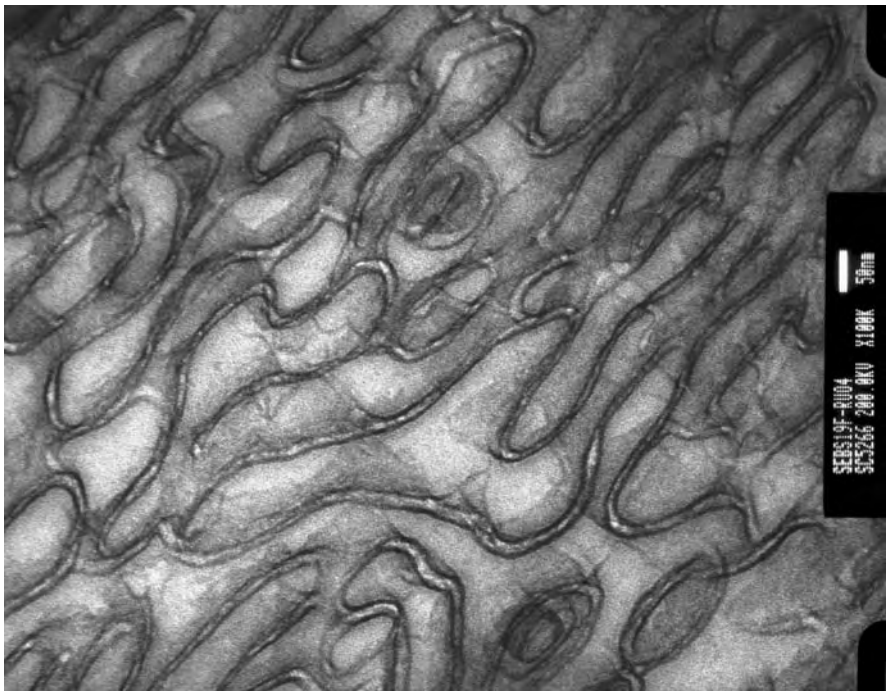

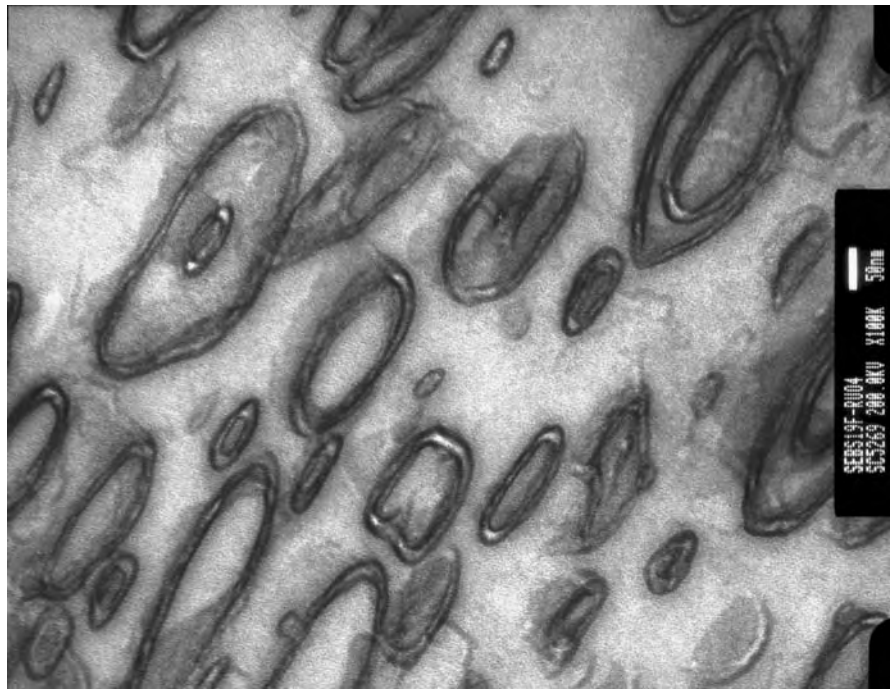

Can't tell "inside" from "outside"

"Inside" and "outside" are distinct, but notice vesicles inside vesicles

Dynamics of polymer membranes

QuickTime™ and a
YUV420 codec decompressor
are needed to see this picture.

Simulation from IBM Almaden website (?Farid Abraham?)

Dynamics of “dilute” polymer membranes via XPCS

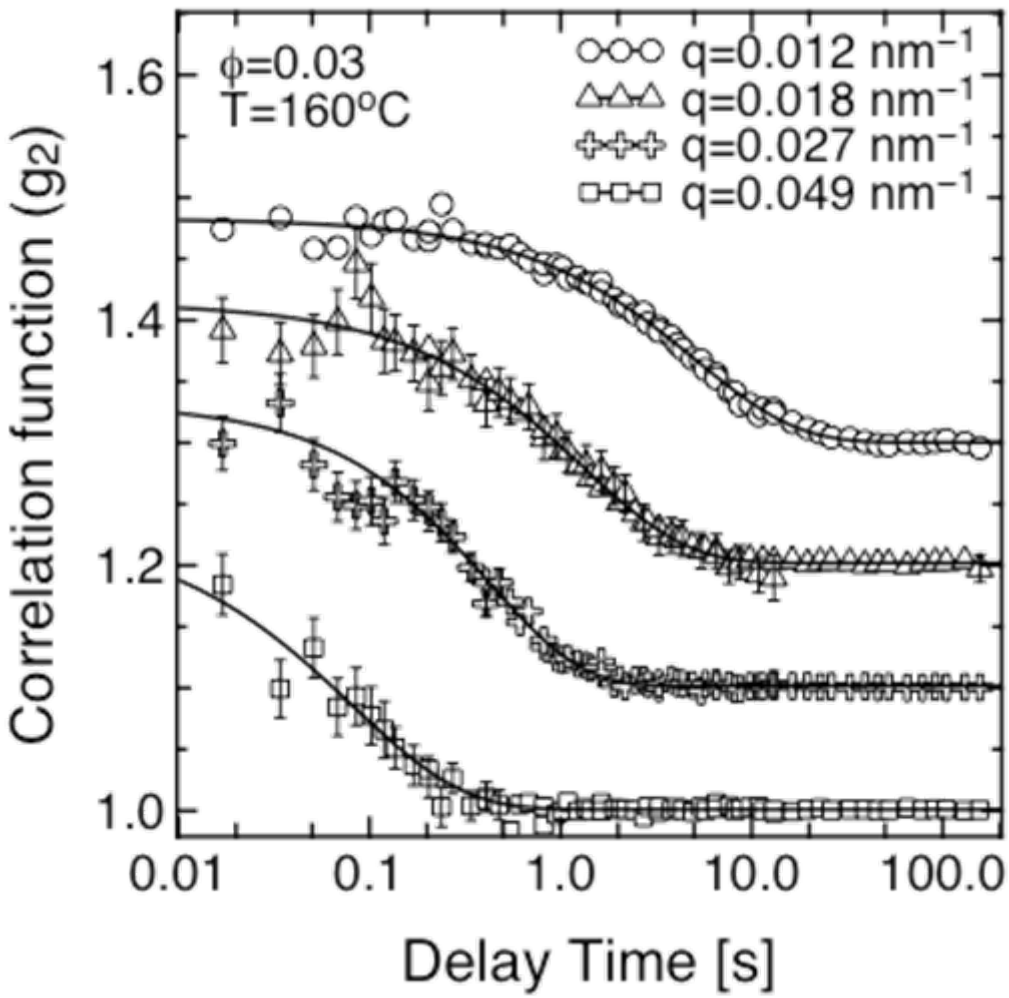

Intensity autocorrelations for a 0.03 SEBS volume fraction sample at 160 C at several wavevectors.

Dynamics of dilute polymer membranes: Zilman and Granek and Frey and Nelson predictions

For individual membranes Zilman and Granek [PRL 77 4788 (1996), Chemical Physics 284, 195 (2002)] [see also Frey and Nelson, J. de Phys. I 1, 1715 (1991)] predict that

$$\Gamma = 0.025(k_B T/\kappa)^{1/2}(k_B T Q^3/\eta)$$

$$f(Q,t) = \exp[-(\Gamma t)]^{\beta}$$

with $\beta = 2[1+k_B T/4\pi\kappa)]/3$ i.e. slightly larger than 2/3!

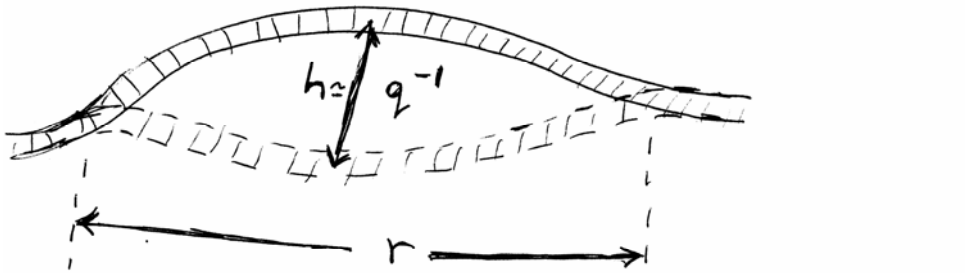

$$\langle h^2 \rangle \simeq \frac{k_B T}{\kappa} r^2 \quad \text{via equipartition}$$

$$r \simeq \left(\frac{\kappa}{k_B T}\right)^{1/2} q^{-1}$$

$$D \simeq \frac{k_B T}{\eta r} = \frac{k_B T}{\eta}\left(\frac{k_B T}{\kappa}\right)^{1/2} q$$

$$\Gamma \simeq D q^2 \simeq \frac{k_B T}{\eta}\left(\frac{k_B T}{\kappa}\right)^{1/2} q^3 \simeq \frac{k_B T}{\eta} q^3$$

DYNAMICS OF ISOLATED MEMBRANES

Membrane undulations are naturally specified by giving the membrane's height (h) above some arbitrary plane whose normal is parallel to the membrane's mean surface normal. These undulations are controlled by an effective Hamiltonian

$$H = \frac{1}{2}\kappa \int d^2r[\nabla^2 h(r)]^2 = \frac{1}{2}\kappa \Sigma_k k^4 h_k h_{-k} \tag{11}$$

This leads to a relaxation rate for a mode of wavenumber k of

$$\Gamma_k = \frac{1}{4\eta k}\kappa k^4 = \frac{\kappa k^3}{4\eta} \tag{12}$$

i.e. the product of a kinetic coefficient (here the Oseen interaction in k-space) and an inverse suspectibility to height fluctuations.

It follows that

$$< h_k(t) h_{-k}(0) >= \frac{k_B T}{\kappa k^4} e^{-\Gamma_k t} \tag{13}$$

and

$$< [h(r,t) - h(r',0)]^2 > \simeq \frac{k_B T}{4\pi\kappa}(r-r')^2 \log(\xi/|r-r'|) + \left[0.069(\frac{k_B T}{\kappa})^{1/2}\frac{k_B T}{\eta}t\right]^{2/3}. \tag{14}$$

DYNAMICS OF ISOLATED MEMBRANES (cont.)

The ISF is related to the height difference via

$$S(q,t) = \frac{1}{a^4}\int d^2r \int d^2r' e^{iq_{\|}.(r-r')} e^{-q_z^2<[h(r,t)-h(r',0)]^2>} \simeq S(q) e^{-[0.025(k_BT)^{3/2}q_z^3 t/(\kappa^{1/2}\eta)]^{2/3}}. \tag{15}$$

This is for a membrane with surface normal along z.

Averaging over orientations gives

$$S(q,t) \simeq S(q) e^{-(\Gamma_q t)^{\beta}}, \tag{16}$$

with $\Gamma_q = 0.025(k_BT)^{3/2}q^3/(\kappa^{1/2}\eta)$ and $\beta = (2/3)[1+(k_BT)/(4\pi\kappa)]$.

Dynamics of polymer membranes via XPCS (cont.)

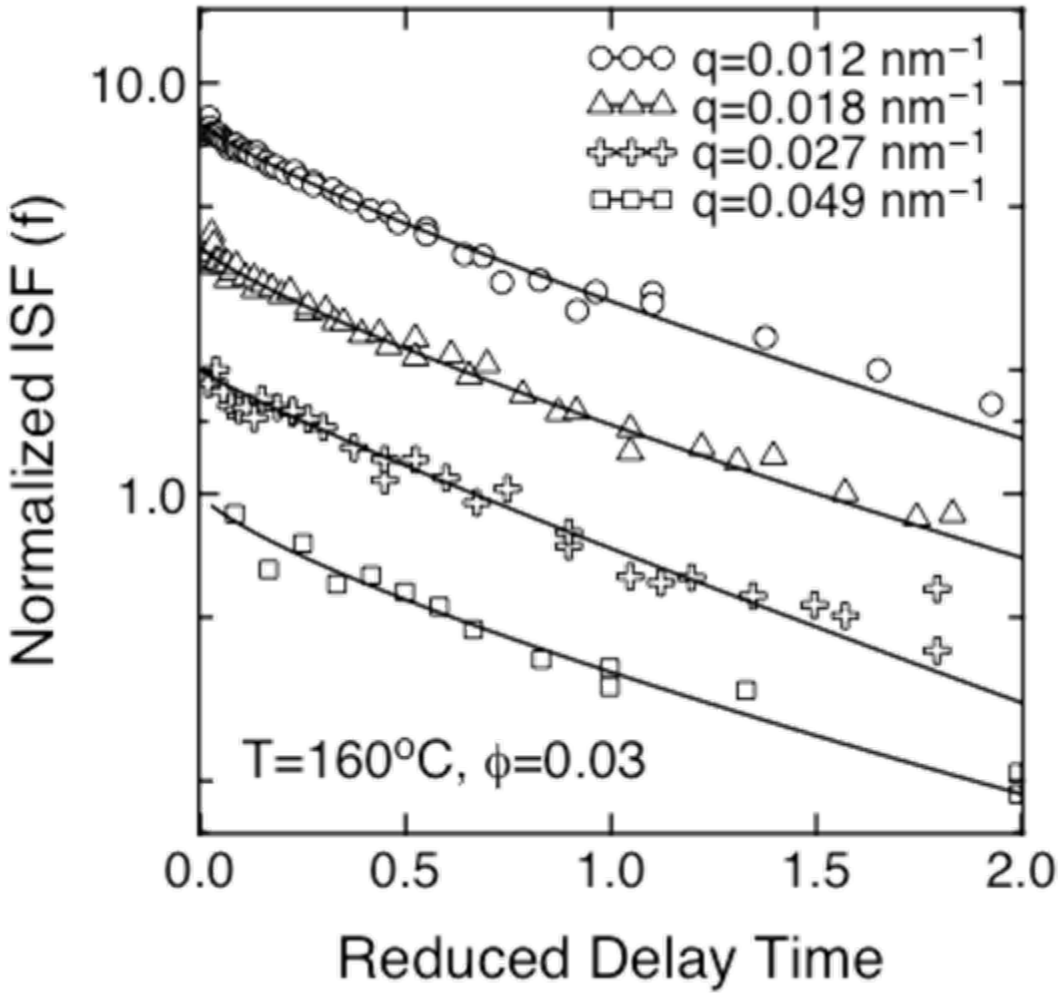

Normalized ISF for a 0.03 SEBS volume fraction sample at 160 C at several wavevectors, plotted so that a single exponential IFS would appear as a straight line, and fitted to a stretched exponential form: $f=\exp[(\Gamma t)^{\beta}]$.

Dynamics of polymer membranes: Fitting results for ϕ=0.03

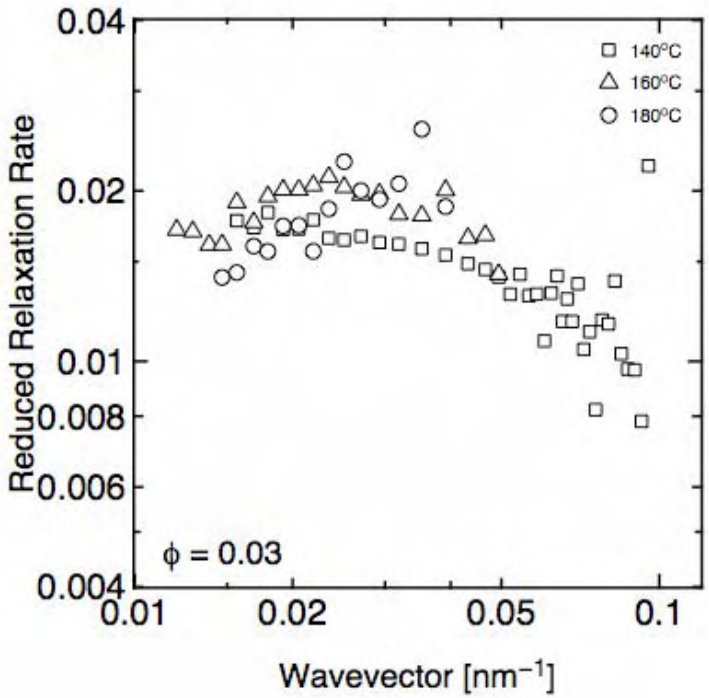

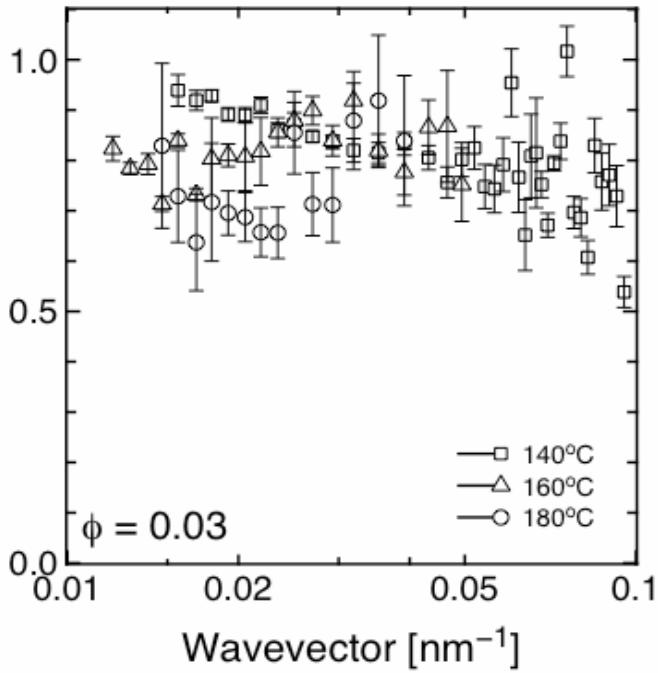

Reduced relaxation rate: $\Gamma/(k_B T Q^3/\eta)$ vs. Q

Sponge phase dynamics: Predictions

Several other groups have proposed theories for the dynamics of sponge phases, applicable at small and intermediate wavevectors.

R. Granek and M. E. Cates, PRA 46, 3319 (1992)
Stretched exponential decays of the ISF , but based on an inappropriate static structure factor.

M. Hennes and G. Gompper, PRE 54, 3811 (1996)
Uses an appropriate structure factor, but finds unstretched exponential decay of the ISF at short times.

M. Nonomura and T. Ohta, J. Chem. Phys. 110, 7516 (1999). Finds single or double exponential decay.

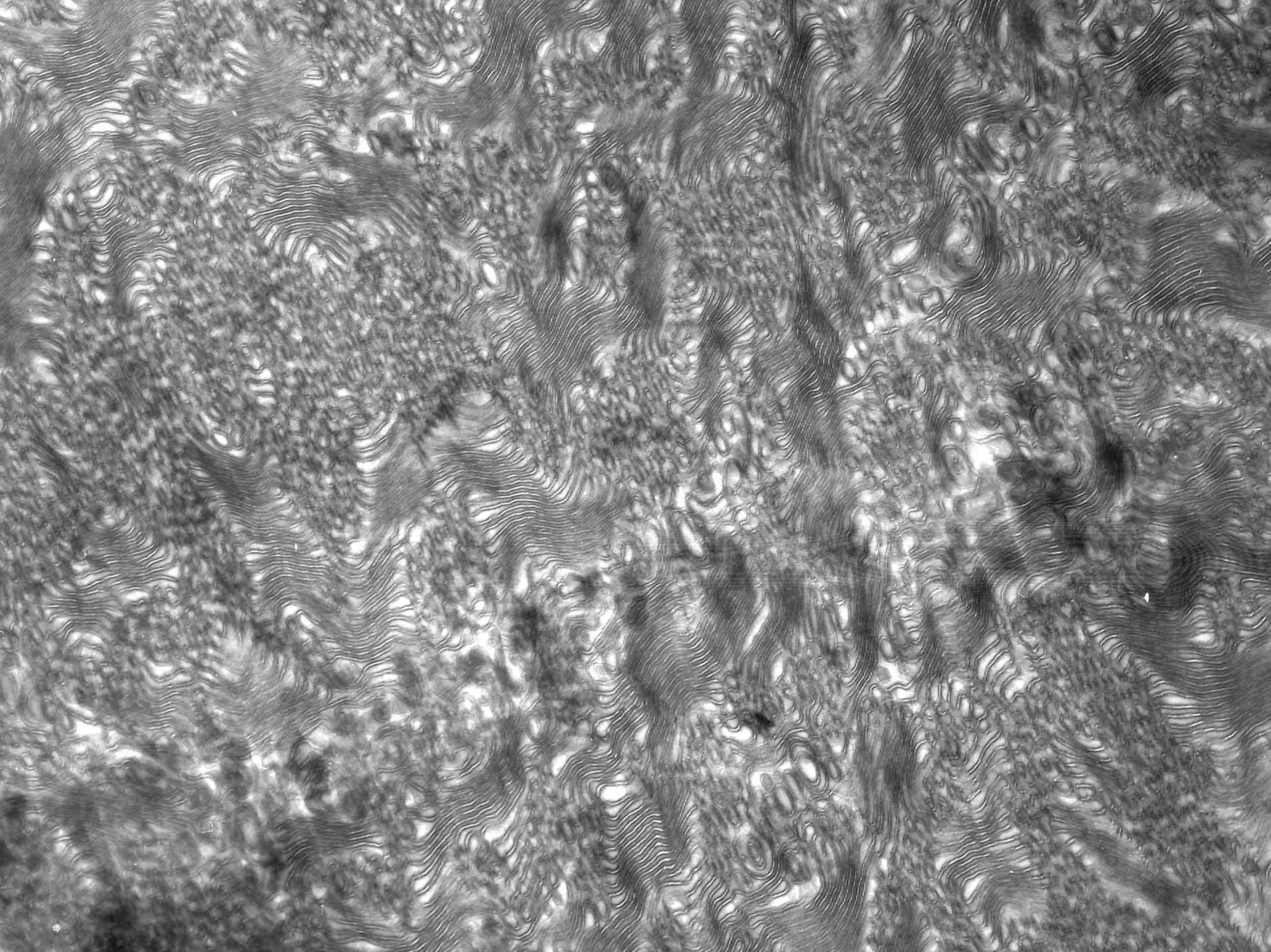

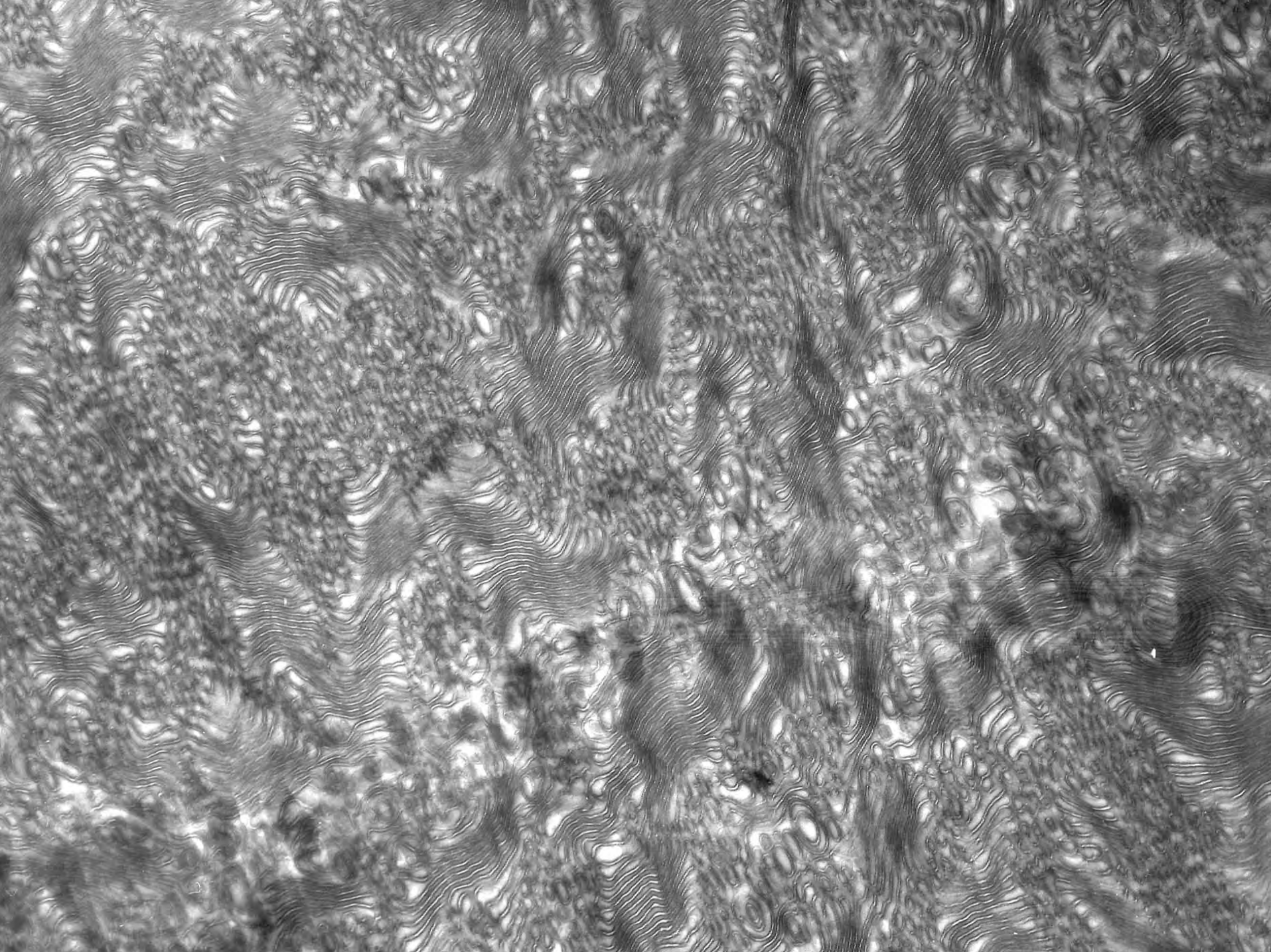

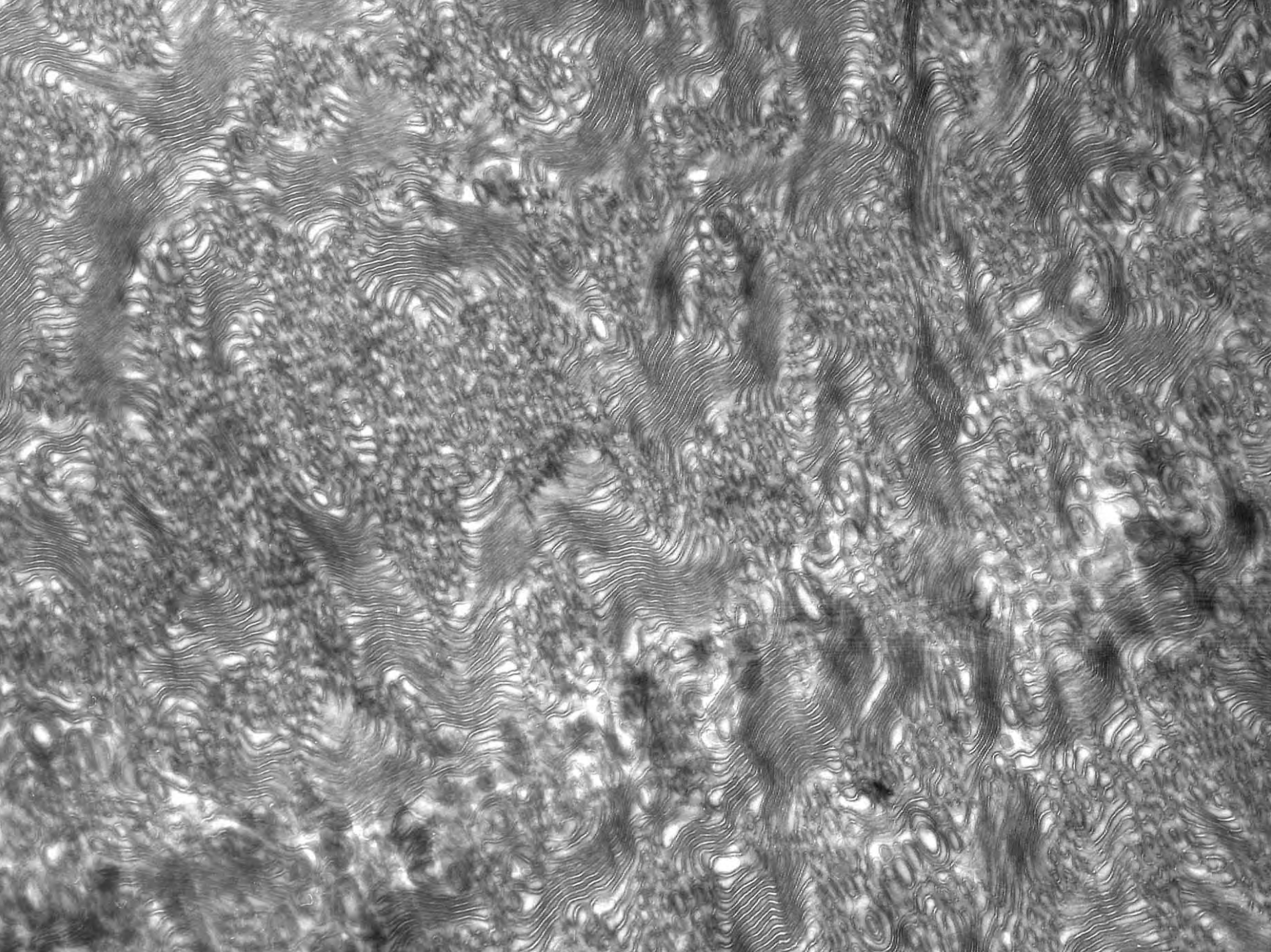

Sponge phase dynamics: Stretching/compression exponent vs. T and Q

What do these results mean?

Usually (in the case of molecular or colloidal glasses), stretched-exponential behavior is associated with transient particle “caging”.

Compressed exponential ISF are unusual, but have recently found for “jammed” systems undergoing “aging”.

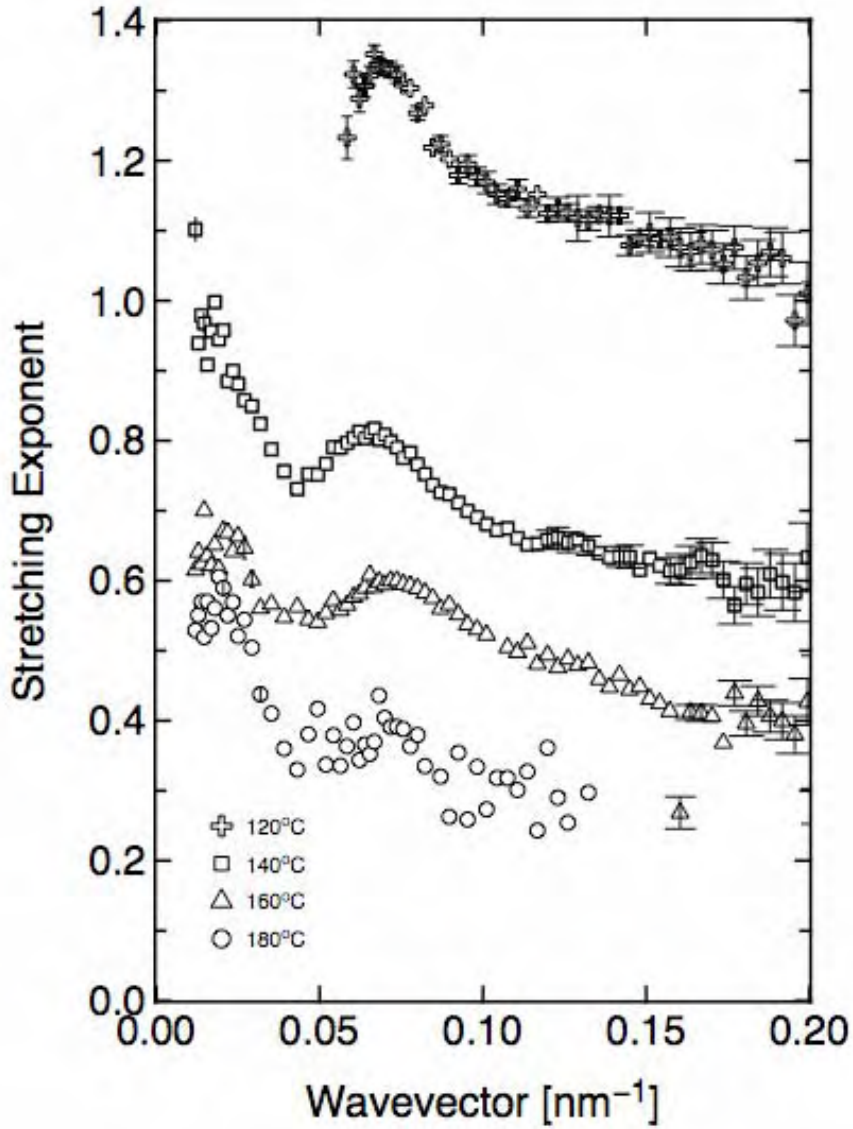

Sponge phase dynamics: De Gennes narrowing

In the stretch exponential regime, there is a minimum in the relaxation rate vs. Q -- this is “de Gennes narrowing”.

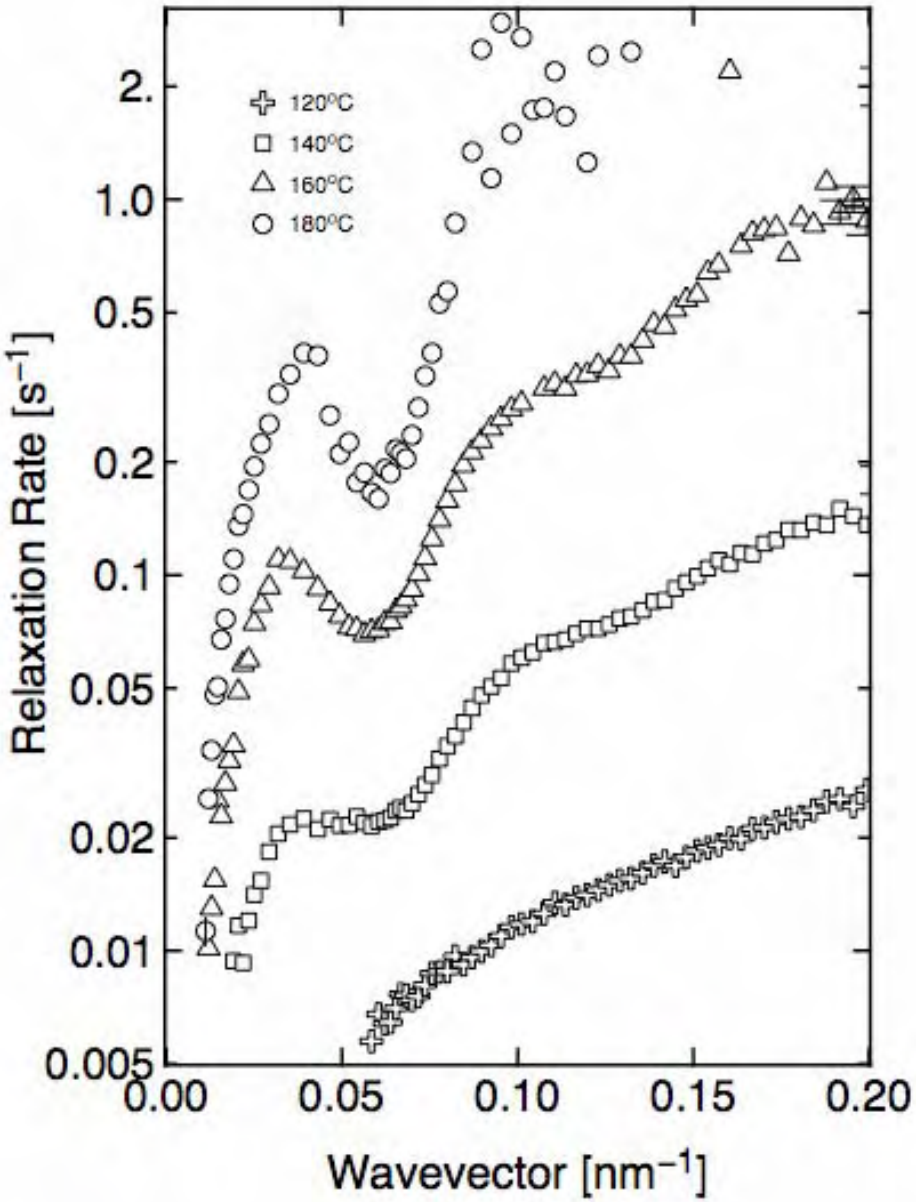

XPCS AT THE ERL

To decide what sorts of experiments will be possible at the ERL, we can scale from 8-ID.

Currently, 8-ID is not fully optimized and we believe that an additional factor of 20 is completely reasonable (vertical focussing, improved detector, etc.)

This means that we can expect an improvement in brightness/SNR of 10^5 in going from 8-ID to an optimized beamline at the ERL.

An important goal for XPCS at the ERL is to achieve short enough time scales to overlap with neutron spin echo i.e. 10^{-7} or less.

Possible XPCS experiments at the ERL:

- Dynamics of block copolymer-based melts of all sorts (straightforward, even at sub-R_G length scales), including under shear to map velocity fields (Wes Burghardt). and solutions (more challenging, but definitely achieveable.) Time scales needed 0.1 s - 0.1 ms.

- Dynamics of lipid and other small-molecule-surfactant membranes and membrane phases in water. Dynamics of Tom Russell's nanoparticle polymerized membranes. Dynamics of fluctuations of ordered complex fluids away from perfect periodicity – "phonon" modes of complex fluids. Time scales needed 1 ms-1 μs. Too slow for NSE.

- Short-length-scale dynamics of membrane AMP pores within stacks of biological membranes, (Gerard Wong and Lin Yang, yesterday) probing pore creation and annihilation times. Membrane protein diffusion within membrane and/or incorporation/rejection times IF slow enough (Time scales unknown.) Similarly, Tom Russell's nanoparticle incorporation/rejection times, IF slow enough i.e. if the nanoparticles are big enough, perhaps 20 nm?

Possible XPCS experiments at the ERL (cont.):

- Short length scale characterization of molecular motors. e.g. kinesin on a microtubule network or immobilized flagella rotary motors. How do the motors actually move? From tweezers experiments, we know a lot, but not the molecular details. Stepping rates are 1 s-1 ms.

- Dynamics of molecular/polymeric glasses on molecular length scales in the previously structurally uncharacterized regime from 0.1 μs to 100 s or longer. 10^4 shorter time scales than at the third generation.

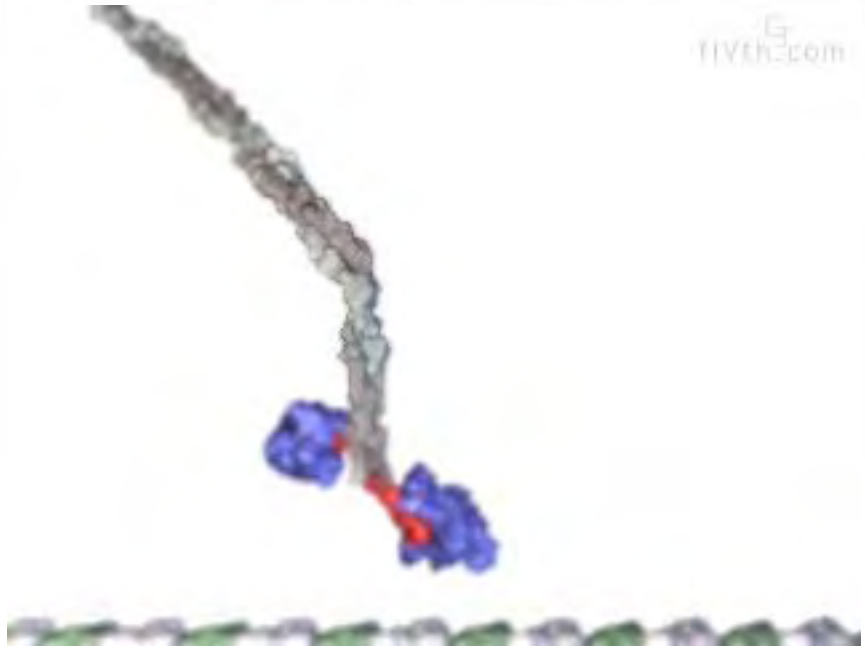

XPCS BEAMLINES AT THE ERL

Creating an optimized XPCS beamline at the ERL is a complicated calculus, but *the* pivotal component is the detector in that the detector characteristics drive much of the beamline optics and layout.

Desirable detector characteristics include:

1. high speed (Determines the fastest processes that can be studied.)

2. high efficiency at high energy (higher energy means less sample damage)

3. large number of pixels (can be increased with multiple detectors)

4. small pixel size (aids resolution of speckles for coherent detection, but NOT as critical as 1 through 3, because it is always possible to use a pixel-size-defining mask.)

Let's pick a detector with 10^6 85 μm pixels, that is 100% efficient at, say, 12 keV (1 Angstrom) or, better, at 20 keV. TO get more pixels, use multiple detectors.

XPCS BEAMLINES AT THE ERL (cont.)

Working backwards from the detector .....

Let's pick a sample-to-detector distance of 8.5 m and 12 keV. (The bigger the detector pixels, the longer the sample-to-detector distance.)

Then for a speckle size on the detector of about 85 μm, the linear dimensions of the illuminated sample area should be about $10^{-10} \times 8.5/(85 \times 10^{-6}) = 10\mu$m i.e. about 10 microns.

As noted above, it's preferable to have a few speckles per pixel, so let's pick $L = 20$ μm.

For an sample-to-detector distance of 50 m, the coherence length at the ERL is about 400 μm (10 μm source size), i.e. 20 times larger than L.

Therefore, an XPCS beamline at the ERL should include focussing to create a virtual source nearer the sample [NOT (probably) at the sample], with a coherence length at the sample of, say, 20 μm. e.g. Place a 5:1 focussing element at 45 m from the source to create a virtual source at 54 m of size 2 μm. Then locate the sample at 54.4 m, where the modified coherence length will be 20 μm.

XPCS BEAMLINES AT THE ERL (cont.)

Upstream of the focussing element, for experiments at larger wavevectors a monochromator seems desirable.

Experience at 8-ID (Narayanan, Sandy, Sprung et al.) suggest a double crystal Ge(111) monochromator is suitable.

Experience at 8-ID also suggests the use of a flat horizontally-deflecting mirror to remove higher harmonics and associated heat load that then no longer needs to be taken by the monochromator.

Before the mirror, a mask and slits should be used to limit what is passed to the beamline to only the useful central cone of undulator radiation.

XPCS BEAMLINES AT THE ERL (cont.)

For many soft matter experiments, it will be essential to address the problem of possible sample damage and incorporate schemes to avoid sample damage right from the start.

But to make meaningful XPCS measurements, it is necessary to illuminate a particular region of the sample for only a few times the sample's correlation time. (XPCS still provides statistical information)

This suggests a sample flow/sample translation scheme that effectively moves a new sample into the beam on a time scale that is slow compared to the sample's correlation time, but fast compared to the sample's damage time.

Finally, already the data rate at 8-ID with a framing camera is an issue at 8-ID (100 Mbyte per second), and we now spend more time on data storage than data acquisition. This suggests that real time data reduction (to pixel g2s) at the ERL, or even a hardware correlator on each pixel.